17th Annual Meeting of the Bulgarian Section of SIAM
December 20 – 22, 2022
Sofia

BGSIAM'22

EXTENDED ABSTRACTS

HOSTED BY THE JOINT INNOVATION CENTRE
BULGARIAN ACADEMY OF SCIENCES

17th Annual Meeting of the Bulgarian Section of SIAM
December 20 – 22, 2022, Sofia

BGSIAM'22 Extended abstracts

ISSN: 1313-3357 (print)
ISSN: 1314-7145 (electronic)

Printed in Sofia, Bulgaria

PREFACE

The Bulgarian Section of SIAM (BGSIAM) was formed in 2007 with the purpose to promote and support the application of mathematics to science, engineering and technology in Republic of Bulgaria. The goals of BGSIAM follow the general goals of SIAM:

- To advance the application of mathematics and computational science to engineering, industry, science, and society;
- To promote research that will lead to effective new mathematical and computational methods and techniques for science, engineering, industry, and society;
- To provide media for the exchange of information and ideas among mathematicians, engineers, and scientists.

During the BGSIAM'22 conference a wide range of problems concerning recent achievements in the field of industrial and applied mathematics will be presented and discussed. The meeting provides a forum for exchange of ideas between scientists, who develop and study mathematical methods and algorithms, and researchers, who apply them for solving real life problems.

The strongest research groups in Bulgaria in the field of industrial and applied mathematics, advanced computing, mathematical modelling and applications will be presented at the meeting according to the accepted extended abstracts. Many of the participants are young scientists and PhD students.

LIST OF INVITED SPEAKERS:

- Nikola Kasabov (Auckland University of Technology, New Zealand)
  "Challenging Problems in Biomedical Data Science and New Opportunities for Applied Mathematics"
- Dimiter Prodanov (Interuniversity Microelectronics Centre (IMEC), Leuven, Belgium)
  "Computation of the Wright function from its integral representation"

The present volume contains extended abstracts of the presentations (Part A) and list of participants (Part B).

Ivan Georgiev
Chair of BGSIAM Section

Hristo Kostadinov
Vice-Chair of BGSIAM Section

Elena Lilkova
Secretary of BGSIAM Section

Sofia, December 2022

Table of Contents

Part A
Extended abstracts[1]

[1] Arranged alphabetically according to the family name of the first author.

Population Dynamics Identification by Lagrange Multipliers Optimization

A. Atanasov, S. Georgiev, L. Vulkov

The parameter estimation is referred to as the inverse modelling problem. It means adjusting the parameters of a mathematical model to reproduce the measured data. Approaches involving inverse problems could be successfully applied to a variety of important processes, including the dynamics of a honeybee population. Although the development of the electronic technology, very often the beekeepers are not able to provide sufficient observation data for modelling the honeybee population. In such a case of scarce data, it is the choice of the mathematical tool that is very important.

Many papers analyzed mathematical models that explored the dynamics of honeybee population, but few of them have been used to predict the optimal parameters of the process development. One of the most prominent population models is suggested in [2] and transformed in its present form in [1], describing the class of young female hive bees H, which work in the hive, and the class of the mature forage bees $\mathcal{F}$, which fly outside the hive. Every bee could be classified into one of the two classes and they do not overlap. The total number of bees is hence $N = H + \mathcal{F}$.

The dynamics of the total number of bees could be described as

$$\frac{\mathrm{d}N}{\mathrm{d}t} = L\frac{N}{\omega + N} - m\mathcal{F}, \tag{1}$$

where L is the maximal queen's laying rate and it is multiplied by a saturation expression in the first term of (1). This term basically represents the eclosion, or how the latter depends on the total number of bees. The constant ω determines how the eclosion approaches the maximal laying rate as N gets large. The other term in (1) represents the foragers death rate. The hive bees mortality is very low and it is neglected.

The population dynamics of the forage bees is given by

$$\frac{\mathrm{d}\mathcal{F}}{\mathrm{d}t} = \alpha N - (\alpha + \sigma + m)\mathcal{F} + \sigma\frac{\mathcal{F}^2}{N}, \tag{2}$$

where α is the maximal rate of which the hive bees are recruited to the forager class and σ describes the social inhibition. When there is no or little foragers, the recruitment rate is high, and vice versa – when there are a plenty of foragers, the recruitment is inhibited by a pheromone-mediated system. It is also possible (although unusual) forage bees to come back to hive duties.

The parameters m, α and σ from (1),(2) are very crucial for the population dynamics, and in the same time they are not directly measurable in practice. That is why it is of high interest to find their 'fair' values via solving inverse identification problems.

We consider the parameter recovery of model (1),(2), but if we only have observations for the hive bees

$$\{H(t^i)\},\ i = 1, \ldots, n,\ t_0 = t^1 < \cdots < t^n = t_{\mathrm{f}}. \tag{3}$$

If the model (1),(2) is given in the form

$$\frac{\mathrm{d}\mathbf{u}}{\mathrm{d}t} = \mathbf{g}(\mathbf{u}, \mathbf{p}), \quad \mathbf{u}(0) = \mathbf{u}_0, \tag{4}$$

where t denotes the time, the m-dimensional vector $\mathbf{p} = \mathbf{p}(t)$ contains all unknown parameters and $\mathbf{u} = \mathbf{u}(t)$ is an n-dimensional vector with the state variables (e. g. number of the hive bees H or number of foragers $\mathcal{F}$), and $\mathbf{g}$ is a given vector function, then the first order minimization necessary conditions are given by

$$\mathcal{A}(v - \mathcal{A}^\top \mathbf{u}) + \dot{\lambda} + \frac{\partial \mathbf{g}^\top}{\partial \mathbf{u}} \lambda = 0, \tag{5}$$

$$\mu \ddot{\mathbf{p}} + \frac{\partial \mathbf{g}^\top}{\partial \mathbf{p}} \lambda = 0, \tag{6}$$

$$\dot{\mathbf{u}} = \mathbf{g}(\mathbf{u}, \mathbf{p}) \tag{7}$$

with the appropriate boundary conditions

$$\mathbf{u}(0) = \mathbf{u}_0, \quad \lambda(\mathrm{f}) = 0, \quad \mathbf{p}(0) = \mathbf{p}_0, \quad \dot{\mathbf{p}}(\mathrm{f}) = \ddot{\mathbf{p}}(\mathrm{f}) = 0, \tag{8}$$

where v is the vector of (non-)linear observations (3), and λ is the vector of Lagrange multipliers.
The suggested computational algorithm recovers a certain set of time-varying parameters, complying with the smallness of the discrepancy between the theoretical quantities and the observed values in practice.

References

[1] A.Z. Atanasov, S.G. Georgiev, Parameter Identification Modeling Honey Bee Colony Population Dynamics, AIP Conf. Proc., 2333, (2021), 090007.

[2] D.S. Khoury, M.R. Myerscough, A.B. Barron, A quantitative model of honey bee colony population dynamics, PLoS ONE, 6(4), (2011), e0018491.

KEDE (KnowledgE Discovery Efficiency): a Measure for Quantification of the Productivity of Knowledge Workers

D. Bakardzhiev, N. K. Vitanov

We discuss problem for the quantification of the productivity of knowledge workers. We introduce a measure of this productivity called $KEDE$ (KnowledgE Discovery Efficiency). The main application of $KEDE$ can be for performance improvement. Then $KEDE$ is extended to account for errors in knowledge discovery and for the lost time in a working day. Characteristic features of $KEDE$ are discussed.

References

[1] Drucker, P. F. (1999). Knowledge-Worker Productivity: The Biggest Challenge. California Management Review, 41 (2), 79 – 94.

[2] Ramirez, Y. W., Nembhard, D.A. (2004) Measuring Knowledge Worker Productivity: A Taxonomy. Journal of Intellectual Capital, 5, (4), 602 – 628.

[3] Leung. Y. (2010). Knowledeg Discovery in spatial data. Springer, Berlin.

A Predictor-Corrector Approach for the Numerical Solution of General Fractional Differential Equations

I. Bazhlekov, E. Bazhlekova

The Adams-type predictor-corrector method for the numerical solution of fractional differential equations proposed by K. Diethelm *et al.* [1] is extended in the present study to equations with general fractional derivative. The method can be used both for linear and nonlinear problems.

Consider the Cauchy problem for the nonlinear general fractional differential equation:

$$({}^{C}D_{t}^{(\kappa)}y)(t) = f(t, y(t)), \quad t \in (0, T], \tag{1}$$

subject to the initial condition

$$y(0) = y_0. \tag{2}$$

Here ${}^{C}D_{t}^{(\kappa)}$ denotes the general fractional derivative of the Caputo type, introduced in [2] as follows

$$({}^{C}D_{t}^{(\kappa)}f)(t) = \frac{d}{dt}\int_0^t \kappa(t-\tau)f(\tau)\,d\tau - \kappa(t)f(0), \;\; t > 0, \tag{3}$$

where $\kappa(t)$ is a nonnegative locally integrable memory kernel, satisfying some additional conditions. Basic examples of memory kernels are the following:

- The power-law memory kernel

$$\kappa(t) = \omega_{1-\alpha}(t) = \frac{t^{-\alpha}}{\Gamma(1-\alpha)}, \quad 0 < \alpha < 1,$$

  where $\Gamma(\cdot)$ is the Gamma function. In this case ${}^{C}D_{t}^{(\kappa)}$ coincides with the Caputo fractional derivative ${}^{C}D_{t}^{\alpha}$ of order α.

- The multi-term power-law memory kernel

$$\kappa(t) = \sum_{j=1}^{m} q_j \omega_{1-\alpha_j}(t), \tag{4}$$

  where $0 < \alpha_j < 1$, $q_j > 0$, $j = 1, \ldots, m$, $m > 1$. In this case

$${}^{C}D_{t}^{(\kappa)} = \sum_{j=1}^{m} q_j \, {}^{C}D_{t}^{\alpha_j}.$$

- The distributed-order memory kernel

$$\kappa(t) = \int_0^1 \omega_{1-\alpha}(t)\mu(\alpha)\,d\alpha, \tag{5}$$

where $\mu(\cdot)$ is a nonnegative weight function. In this case ${}^{C}D_t^{(\kappa)}$ is the Caputo fractional derivative of distributed order:

$$ {}^{C}D_t^{(\kappa)} = \int_0^1 \mu(\alpha) {}^{C}D_t^{\alpha} \, d\alpha. $$

To deduce the predictor and corrector formulae, the following equivalent representation of the problem (1)-(2) as a Volterra integral equation is used

$$ y(t) = y_0 + \int_0^t k(t-\tau) f(\tau, y(\tau)) \, d\tau, \;\; t \in (0, T], \tag{6} $$

where the kernels $k(t)$ and $\kappa(t)$ are a pair of Sonine kernels, i.e. they satisfy the identity

$$ \int_0^t \kappa(t-\tau) k(\tau) \, d\tau = 1. $$

The Volterra integral equation (6) is solved on a uniform mesh in two steps: predictor and corrector step. For the approximation of the integral in (6), the product rectangle rule is used in the predictor step and the product trapezoidal quadrature formula in the corrector step. Numerical examples are given for the particular cases of multi-term and distributed order fractional differential operators, corresponding to kernels (4)and (5), which demonstrate the viability of the developed numerical algorithm.

Acknowledgment. The first author (I.B.) is supported by the Bulgarian National Science Fund under Grant FNI KP-06-H22/2.

References

[1] K. Diethelm, N. Ford, A. Freed, A predictor-corrector approach for the numerical solution of fractional differential equations, *Nonlinear Dynam.*, **29** (2002), 3–22.

[2] A.N. Kochubei, General fractional calculus, evolution equations, and renewal processes, *Integral Equ. Oper. Theory*, **71** (2011), 583–600.

Wave Propagation in Viscoelastic Media of Zener Type

E. Bazhlekova, M. Datcheva, S. Pshenichnov

Rheological constitutive equations involving fractional derivatives in time play an important role in linear viscoelasticity and have a long history [1]. It appears that using fractional derivatives in time, the damping behaviour of viscoelastic media can be modelled with much less parameters, compared to the integer-order models. In linear viscoelasticity the rheological properties of a viscoelastic medium are described through a linear constitutive relation between stress σ and strain ε. In the uniaxial case, in which $\sigma = \sigma(x,t)$ and $\varepsilon = \varepsilon(x,t)$, and considering systems quiescent for all times prior to some starting time, $t = 0$, the constitutive equation admits the form

$$\sigma(x,t) = \int_0^t G(t-\tau)\dot{\varepsilon}(x,\tau)\,d\tau, \quad t > 0, \tag{1}$$

where $G(t)$ is the so-called relaxation modulus and the over-dot denotes the first derivative in time. In a physically meaningful model the relaxation modulus $G(t)$ should be a non-negative and non-increasing function for $t > 0$, which is related to the physical phenomenon of stress relaxation. Often $G(t)$ obeys a stronger property: it is a completely monotone function. A function $f : (0,\infty) \to (-\infty,\infty)$ is said to be completely monotone if it is of class C^∞ and

$$(-1)^n f^{(n)}(t) \geq 0, \quad t > 0, n = 0, 1, 2, ... \tag{2}$$

The Zener constitutive law and its fractional order generalizations are extensively used as models of solid-like viscoelastic behaviour. In the present study we consider the generalized Zener model [2]

$$a\,{}^C D_t^{(\kappa)}\sigma(x,t) + \sigma(x,t) = b\,{}^C D_t^{(\kappa)}\varepsilon(x,t) + \varepsilon(x,t). \tag{3}$$

Here $a > 0, b > 0$ are constants and ${}^C D_t^{(\kappa)}$ denotes a general convolutional derivative in time

$$({}^C D_t^{(\kappa)} f)(t) = \frac{d}{dt}\int_0^t \kappa(t-\tau) f(\tau)\,d\tau - \kappa(t) f(0), \quad t > 0, \tag{4}$$

where $\kappa(t)$ is a locally integrable and completely monotone function.
We prove that when $a < b$ the relaxation modulus $G(t)$, corresponding to the generalized Zener model (3), is a completely monotone function. This fact implies that for equations modeling wave propagation in a viscoelastic medium with constitutive law (3) the so-called subordination principle is satisfied, see e.g. [3]. We apply the subordination principle to derive representation of the solutions to wave equations of this type for different choices of the kernel $\kappa(t)$.

Acknowledgements. This study was performed within the bilateral project funded by the Bulgarian National Science Fund, Project number KP-06-Russia/5 from 11.12.2020 and by the Russian Foundation for Basic Research, Project number 20-58-18002.

References

[1] F. Mainardi, *Fractional Calculus and Waves in Linear Viscoelasticity*, Imperial College Press, London (2010).

[2] T.M. Atanackovic, S. Pilipovic, Zener model with general fractional calculus: Thermodynamical restrictions. *Fractal Fract.* (2022), 6, 617.

[3] E. Bazhlekova, *Subordination Principle for Generalized Fractional Evolution Equations*, D.Sc. dissertation, Institute of Mathematics and Informatics, Bulgarian Academy of Sciences (2022).

Some Properties of the Interest Rate Spread for Expected Risk of Consumer Loans

V. Boutchaktchiev

A loan's interest rate is formed by adding various components to the risk-free rate, including spreads for the various types of risk, cost of capital, and all sorts of expenses the Bank accrues in its daily functioning.
The focus of this study is on the spread for expected credit risk, which is designed to compensate the investor for the estimated risk of default of the debtor.
We assume that the loan contract imposes a continuously compounded interest and provides for continuous repayment. This assumption is rarely satisfied in full. However, the contracts for many consumer loans often call for periodic compound interest with repayment made in regular installments. Our assumption is a close approximation of these conditions and provides the technical ability to simplify the analysis.
We start by computing the *expected credit loss* (ECL) for a given loan, according to the requirements of the IFRS9 accounting standard. The ECL measures the credit quality and is computed using several essential parameters including, Exposure at default, Loss given default, and probability of default. Within the perimeter of our study, these quantities can be interpreted and expressed with explicit functions of the *interest rate*, r and *the term*, T, of the loan.
Furthermore, the relation between r and T is expressed using an equation:

$$g(r, T) = 0,$$

depending on parameters, such as the level of collateralization and probability of default distribution.
Our most prominent result is summed up in the following theorem:

Theorem 1 *Under the previously mentioned reasonable conditions, the interest rate spread for expected credit risk is a decreasing function of the term of the loan.*

This dependence, it turns out, is somewhat counterintuitive, but it is nonetheless confirmed through empirical simulations.

Acknowledgment This work has been supported in part by UNWE Research Program (Research Grant No. 11/2022/A)

References

[1] Dushkov, I. N., Jordanov, I. P., Vitanov, N. K., Numerical modeling of dynamics of a population system with time delay. *Math Meth Appl Sci.* 2018; 41: 8377– 8384. https://doi.org/10.1002/mma.4553

[2] Edelberg, Wendy, Risk-based pricing of interest rates in consumer loan markets. *Finance and Economics Discussion Series* 62, 2003.

[3] Ho, T., and A. Saunders., The determinants of bank interest rate margins: Theory and empirical evidence, *Journal of Financial and Quantitative Analysis*, 16(4), pp. 581–600, 1981.

[4] Iliev, A.I., Emotion Recognition in Speech using Inter-Sentence Time-Domain Statistics, *International Journal of Innovative Research in Science, Engineering and Technology*, Vol. 5, Issue 3, pp. 3245-3254, March 2016,

Anastylosis of Frescos an Optimized Performance on Avitohol HPC

D. Dimov, S. Ivanovska, K. Alexiev, A. Hristov

The RINCCAS method (**R**otation-**I**nvariant **NCC** for 2D Color Matching of **A**rbitrary **S**haped Fragments of a Fresco) was developed at IICT-BAS for participation in the computer competition DAFNE (Digital Anastylosis of Frescos challeNgE), June-July 2019 [1, 2]. DAFNE was organized by the University of Pavia, Italy, and is motivated by the need for efficient digital reconstruction of frescoes from their ruins, i.e. a set of their fragments of random shapes, often less or more damaged by the time and possibly mixed with other, spurious fragments. This is a well-known problem from the practice of world cultural heritage preservation [3].
RINCCAS is built on a classical approach based on normalized cross-correlation (NCC) presented in [4] and implemented in MATLAB (R2010 and higher) through the *normxcorr2*() function, which we mainly modified.
The approach: Complete enumeration of the possible situations of each of the presented fragment images (integer position and rotation) relative to the corresponding fresco image. This approach, often used to solve similar problems, was chosen because:

- The non-linear (non-rectangular) shape of the fragments;
- The presence of random rotation when capturing (scanning) each of the fragments;
- Almost complete lack of peripheral (contour) correspondence between the fragments.

The high accuracy of the results is characteristic of the chosen approach, but it is **at the expense of a significant computational resource**, even for medium-sized tasks of the given type, similarly [3]. Asymptotically, the computation time is of logarithmic-cubic order

$$O(RINCCAS) \sim K(N+n)^2\, n\, log(N+n),$$

where $N^2 = N_x N_y$ reflects the input fresco image area (in pixels), K is the number of fragments, and $n^2 \approx 0.5 \sum_{i=1}^{K} |A_i|/K$ is about a half of averaged area over all fragments, as their curvilinear shapes are approximated by MACIRs (Maximal & Axes-Collinear Inner Rectangles). Memory requirements are more moderate – dependent quadratically on the dimensions (linearly of the area) of the fresco and fragments.

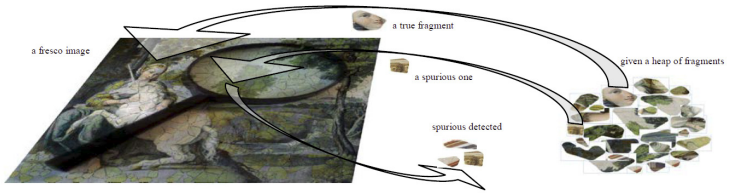

Figure 1: A sketch of the main application of RINCCAS (a graphical abstract [1])

Due to the importance of the application, **we had to adapt RINCCAS to a sufficiently powerful HPC**, like the Avitohol HPC of IICT-BAS. This is how the RINCCAS-HPC project task for building the "Anastylosis of Frescos" web-service under the NI4OS project of IICT-BAS was formulated.
At BGSIAM'22, the experience and results of RINCCAS parallelization, as a method, algorithm and program code, for an attractive web-service to the NI4OS project, will be discussed in the following research aspects:

- **The task parallelisms** is the chosen parallel computing scheme, due to independence between particular sub-tasks, K in number for a given fresco, 1 for the positioning of each of the fragments.
- **Optimal loading of the provided computing resource** of the given HPC. Optimality aims at a minimum time for the execution of an experiment (the overall task) of the type "anastylosis of frescos" while observing given limitations of operational memory.
- **Two main cases of optimal design of experiments:**
  (i) Optimal planning with one node, which at Avitohol is available with up to 16 cores, each with hyper-threading.
  (ii) Optimal planning on several (more than one) Avitohol nodes in parallel.
- **The optimal planning of RINCCAS-HPC experiments** as a specific case of the "knapsack problem" [5].

Acknowledgements This work is supported by the project NI4OS-Europe, National Initiatives for Open Science in Europe, H2020 No 857645.

References

[1] Dimov, D.T. (2020). Rotation-invariant NCC for 2D color matching of arbitrary shaped fragments of a fresco. Pattern Recognit. Lett., 138, 431-438.
[2] Cantoni, V., G.L. Foresti, N. Sebe (2021) Editorial for the special issue on the DAFNE project (Digital Anastylosis of Frescoes challeNgEc, Pattern Recognition Letters, 147, July 2021, 179-180.
[3] Fornasier, M., Toniolo, D. (2005). Fast, robust and efficient 2D pattern recognition for re-assembling fragmented images. Pattern Recognit., 38, 2074-2087.
[4] Lewis, J. P. (1995). Fast Normalized Cross-Correlation
[5] Martello, S., Pisinger, D., Toth, P. (1999). Dynamic Programming and Strong Bounds for the 0-1 Knapsack Problem. Management Science, 45, 414-424.

Custom Markers for 3D Laser Scanning of Architectural Heritage and Archaeology

G. Evtimov, D. Dimitrov

$3D$ laser scanning is increasingly entering the architectural heritage, archaeology and constructions. With this method easy can make documentation of cultural monuments. $3D$ laser scanning is a representing real objects in a virtual environment. In this article the focus will be on $3D$ laser scanning of architectural heritage and archeology sites. For brevity we will call them objects.

For this purpose, we will use a FARO Scan Focus+ scanning device. 3D laser scanning technology allows us to scan objects by obtaining a cloud of points. A cloud of points represents multiple points with tree coordinates x, y, z as well as three values for the color of the each point R, G, B. So for one point the record is x, y, x, R, G, B. The accuracy is 2 mm (distance between points) in high precision mode and 15mm (distance between points) in low precision mode.

The given survey object is done by placing the device at several positions around the object. All point clouds have to be aligned relative to each other. Alignment of point clouds can be done in several ways:

1. Through geodesic points with calculated point coordinates. The minimum number of geodesic points are three;
2. Through markers. The markers can be $2D$ or $3D$;
3. Visually - by finding common edges that are the same in two or more point clouds.

Here we will use the second method - using markers. Correctly placed markers on the site object, will be more accurately align the point clouds relative to each other. Markers must be placed in a visible area of the scanner. If markers are viewed from a greater number of positions, all point clouds will align more accurately. For objects with many and small details, a local scan are made with a higher resolution of the scanned device. The resulting is many point clouds. They will be aligned to the total point cloud. For alignment is using $2D$ or $3D$ markers. Once the overall point cloud is obtained, the model can be easily converted into an STL file for printing on a 3D printer. Laser scanning allows us to accurately capture complex architectural heritage and archeological excavations.

The Application of Region Growing as a Segmentation Method in Micro CT Studies in Endodontics

I. Georgiev, M. Raykovska

Introduction Micro-X-ray computed tomography finds application in various fields such as science, industry, etc. This comprehensive method allows in a non-destructive manner to reach details that are impossible to analyse with other approaches. In dentistry, microcomputed tomography allowed for the first time the establishment of large-scale studies of the root canal anatomy and treatment features of this complex system. Currently, Micro-CT technology is considered the most important and accurate method for studying the root canal system and, among other applications, understanding the influence of its complex morphology on the different stages of endodontic treatment [1].
This presentation aims to demonstrate the Region growing segmentation method and its application in endodontic research. It is a segmentation procedure that groups voxels into larger regions. The logic behind this algorithm is the principle of similarity. That means that all the Region's pixels have the same grey level. The selection of the initial seed, the seed growing criteria and the segmentation process's termination is essential. After the initial seeding, the Region grows three-dimensional by merging neighbouring voxels. The end of the growth is when the border of the Region meets the edge of another region [2].

Materials and methods Twelve teeth were selected from a storage bank of extracted teeth for periodontal reasons, and all the patients signed an informed consent authorising their examination. The specimens were scanned in four stages, repeating the stages of the endodontic procedure - respectively, steps that are fundamental to research in Endodontics. The first scan is of teeth where the pulp space has not been entered and the anatomy has been preserved. Secondly, the teeth were scanned after opening the pulp chamber and instrumenting the root canal. The third stage of scanning is after the root canal obturation procedure, and the fourth is after retreating the filling material. The samples were scanned with a Nikon XT H 225 system developed by Nikon Metrology. With continuous rotation, 2525 digital radiographic projections were acquired. The Inspect-X CT software was used to control the acquisition process. Sample scanning was performed with a voltage of $100kV$, a tube current of $110\mu A$ tube current, and an exposure time of $500ms$. The size of the voxel was $10\mu m$. Volume reconstructions were performed using CT Pro 3D software developed by the equipment producer. Volume rendering, porosity analysis, and measurements were performed using the VGStudio Max 2.2 software from Volume Graphics Inc., Heidelberg, Germany. The chosen segmentation was Region Growing.

Results After the acquisition and reconstruction process, forty-eight tooth models were created representing different stages of root canal treatment. The resulting Histogram of the samples is bi or three-modal, which means the different shades of grey are clearly defined with visible borders. The segmentation was achieved in all specimens.

Acknowledgments The financial support provided by the Bulgarian National Science Fund, grant KP-06-H27/6 from 08.12.2018 (I.G.) is gratefully acknowledged.

References

[1] Versiani MA, Keles A.; Applications of micro-CT technology in endodontics. In: Orhan K, ed. Micro-computed tomography (micro-CT) in Medicine and Engineering, 1 st edn. Switzerland: Springer Nature, 2020, pp. 182-211.

[2] Alireza Norouzi, Mohd Shafry Mohd Rahim, Ayman Altameem, Tanzila Saba, Abdolvahab Ehsani Rad, Amjad Rehman & Mueen Uddin (2014) Medical Image Segmentation Methods, Algorithms, and Applications, IETE Technical Review, 31:3, 199-213.

Power Monte Carlo Method Using Randomized Low Discrepancy Sequences

S.-M. Gurova, E. Atanassov, A. Karaivanova

The Power Monte Carlo method is successfully applied for estimating extremal eigenvalues especially those of large sparse matrices. The successful applications of scrambled quasi-random sequences motivate us to apply them to the iterative Monte Carlo approach for the approximate evaluation of the maximum eigenvalue. We propose a new algorithm that uses the iterations of the Power Monte Carlo method for a generated random symmetric sparse matrix. BRODA's Sobol Randomized Sequence Generator (broda.co.uk/software.html) was used for the numerical experiments, providing excellent efficiency when using the GPU accelerators.

Acknowledgements This work has been accomplished with the partial support by the Grant №BG05M2OP001-1.001-0003, financed by the Science and Education for Smart Growth Operational Program (2014-2020) and co-financed by the European Union through the European structural, Investment funds and by a grant №30 from CAF America. The work was accomplished with the financial support of the MES by the Grant №DO1-168/28.07.2022 for providing access to e-infrastructure of the NCHDC – part of the Bulgarian National Roadmap on RIs.

Effective Material Properties Evaluation via Numerical Homogenization and Microstructure Testing Data

R. Iankov, I. Georgiev, M. Raykovska, G. Chalakova, M. Datcheva

This work is devoted to a 3D hybrid numerical-experimental homogenization strategy for determination of effective characteristics of materials with voids or inclusions. The performed homogenization procedure employs micro-computed tomography (uCT) and instrumented indentation testing data (IIT).

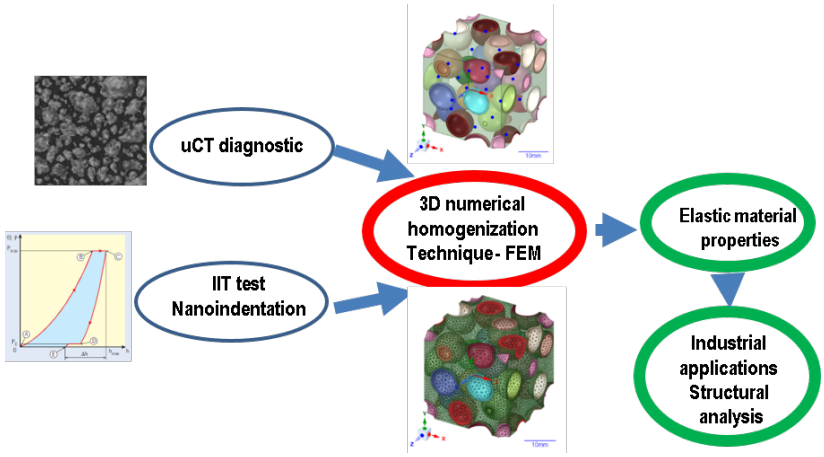

Based on the uCT data a 3D geometrical model of a cubic representative elementary volume (RVE) is created assuming periodic microstructure of the material with inclusions. Creating the RVE respects the following principle of equivalence: the porosity assigned to the RVE is the same as the porosity calculated based on the uCT images. Next, this geometrical model is used to generate the respective finite element model where, for simplicity, the voids are considered to have a spherical form. The numerical homogenization technique includes proper periodic boundary conditions with unit force applied in normal and shear directions. The employed constitutive model for the solid phase is the linear elastic model whose parameters are determined based on IIT data. It is performed a validation and verification study using simplified geometries for the RVE and under different assumptions for modelling the voids.

Acknowledgement The financial support provided by the Bulgarian National Science Fund, grants KP-06-H27/6 /08.12.2018 (I.G.) and by the Science and Education for Smart Growth Operational Program (2014-2020) and the European Structural and Investment Fund through grant BG05M2OP001-1.001-0003 (M.D.) is gratefully acknowledged. We also acknowledge the provided access to the infrastructure of the Laboratory for Nanostructure Characterization, financed by by the Science and Education for Smart Growth Operational Program (2014-2020) and the European Structural and Investment Fund, grant BG05M2OP001-1.001-0008.

Wave Propagation Through a Viscoelastic Layer with Uniformly-Distributed Elastic Inclusions

R. Ivanov, S. Pshenichnov, M. Datcheva

Some natural materials like soil have inherent viscoelastic properties, and also randomly distributed inclusions such as rocks and boulders. In man-made materials, often alteration of the properties is sought by techniques like functional grading, introducing of inclusions or layering of different materials to achieve a practical goal. This may be tuning the propagation of waves, so that strong attenuation is achieved at particular locations. In [1] a numerical study of surface wave propagation in an elastic matrix with different shape and size of thin inclusions is carried out, and is found that the longitudinal and Rayleigh wave velocity change almost up to 15% depending on the inclusion shape. In [2] the effect of inclusion shapes, inclusion contents, inclusion elastic constants, and plate thickness on the dispersion relations and modes of wave propagation in inclusion-reinforced composite plates is examined. It is found that propagation speed is generally increased with the aspect ratio, e.g., using longer fibers generally results in a higher propagation speed. In [3] it is found that specimens with a volume fraction of rigid inclusion equal to 70% have a Vs up to 250% higher than the same soil without inclusions when the vertical stress is low. These are just some of multitude of studies with often unexpected and intriguing results.

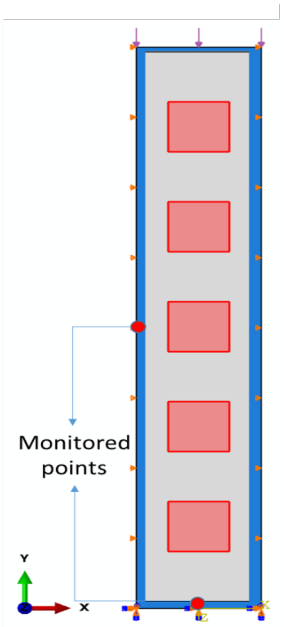

Fig. 1. FEM model

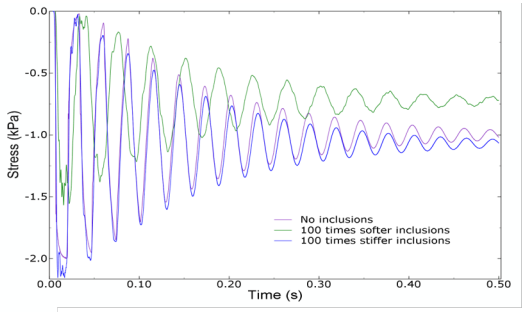

Fig. 2. Vertical stress at the bottom

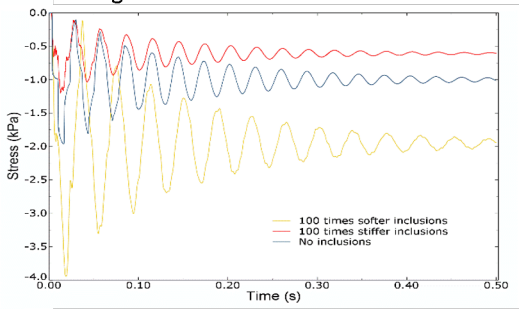

Fig. 3. Vertical stress at the left

This study is a continuation of previous ones whereby the performance of FEM and more

specifically the commercial software package ABAQUS [4] was verified against theoretical solutions of problems of wave propagation through viscoelastic media. Here we study the effect of elastic inclusions on the P-wave propagation through a viscoelastic layer subjected to a smoothed-step normal stress pulse applied on the surface. The inclusions are square in shape and are uniformly distributes through the volume of the layer in a square pattern. Due to symmetry, only one column of inclusions with the surrounding layer (matrix) is modelled. The model is fixed at the bottom, and restrained to move laterally at its left and right sides, Fig. 1. The matrix has a Young's modulus of 30 GPa, Poisson ratio of 0.3 and density of 2.4 ton/m3. The inclusions have the same Poisson ratio as the matrix, the density is taken as 1 ton/m3 when the inclusions are softer than the matrix and 7.8 when harder than the matrix. The Young's modulus of the inclusions was varied from 1/1000 to 100 times the modulus of the matrix. The normal longitudinal stresses at the middle of the bottom side and the middle of the left/right side we monitored and the results compared. The results of the stress at the bottom are shown in Fig. 2 and those at the left side in Fig. 3. It can be seen that with stiffer inclusions the stress at the in the middle of the base is larger than in the case without inclusions, and the reverse is true for the case of softer inclusions, Fig. 2. The effect of softer inclusions is much more pronounced however. The reduction of the waver propagation speed with softer inclusions is also significant while for while with stiffer inclusions the wave speed practically does not change. The differences in the response are much more pronounced for the middle of the left side, Fig. 3. With softer inclusions the stress concentration is obvious and the factor of concentration is close to 2, as is should be if the inclusions were void. On the other hand, significant stress alleviation occurs with stiffer inclusions.

Acknowledgement This study was performed within the bilateral project funded by the Russian Foundation for Basic Research (RFBR), project number 20-58-18002 and by the Bulgarian National Science Fund, project number KP-06-Russia/5 from 11.12.2020.

References

[1] D.G. Aggelis, "Numerical simulation of surface wave propagation in material with inhomogeneity: Inclusion size effect", NDT&E International, vol. 42, 2009, pp. 558-563. doi: 10.1016/j.ndteint.2009.04.005

[2] Y.C. Liu, J.H. Huang, "Dispersion relations and modes of wave propagation in inclusion-reinforcedcomposite plates", Composites: Part B, vol. 43, 2012, pp. 1649-1657,
doi: 10.1016/j.compositesb.2012.01.018

[3] G.O. Bogado, F.M. Francisca "Shear wave propagation in residual soil–rigid inclusion mixtures", Powder Technology, vol. 343, 2019, pp. 595-598.
doi: 10.1016/j.powtec.2018.11.074

[4] Dassault Systemes Simulia Corp, ABAQUS Analysis User's Manual 6.12-13, 2012.

Generation of Secure Public-Verifiable Random Numbers

J. Jeliazkov, H. Kostadinov

Generation of security-relevant random and pseudo-random numbers is a key element of modern security systems.
There are several non-IT cases, where real-life processes are significantly relying on a random choice.
Some examples start from a random coin flip at the beginning of a football match to the random selection of judges in court.
The more significant the choice is, the higher are the chances that one or more of the involved parties will be tempted to influence the outcome of the generation to get more favorite results.
In some publicly visible areas, the historical data about the random choice is statistically impossible to be random.
Such data is a clear indication that these processes are influenced and corrupt.
In this study we demonstrate a method random selection that is completely public and use a well-known selection method that may not be tempered with (directly or indirectly).
This method is implemented by using public blockchain technology to guarantee publicity and traceability of the selection process.

Application of the Simplest Equations Method to Logarithmic Schrödinger Equation

I. P. Jordanov

The dynamics of many social and economic systems is nonlinear. During the past few decades many non–linear phenomena are modeled by systems of nonlinear partial differential equations (PDEs). Such model systems require applications of the methods of non–linear dynamics, chaos theory, and theory of stochastic processes In more detail, reaction-diffusion equations have many applications for description of different kinds of processes in physics, chemistry, biology, economics and social sciences. The most systems in our environment contain components that interact through competition or cooperation which at some cases can lead to adaptation of the interactions. It is of special importance to study the behavior of such systems, and to develop and apply new appropriate mathematical methods for description of processes in these systems. In addition, the agent models are an important tool for analysis of complex systems Depending on nature of the system, the agents may have variety of properties, as well as they can interact in different ways. In the recent years we observe a rapid growth in publications related to agent models because they may explain adequately the complex processes in a number of social systems, such as migrations of various human populations

In this study we apply the Simple Equations Method (SEsM) [3]-[3] to obtain exact solution of equations which are connected to the nonlinear logarithmic Equation of Schrödinger. The used simple equations are more simple than the solved nonlinear partial differential equation but these simple equations in fact can be quite complicated. We consider the specific case of SEsM for obtaining exact solution of one nonlinear partial differential equation. We use specific case of SEsM which is based on the use of 2 simple equations [4].

Acknowledgments This work contains results, which are supported by the UNWE project for scientific research with grant agreement No. NID NI – 17/2021 and No. NID NI – 22/2023

References

[1] Nikolay K. Vitanov, Zlatinka I. Dimitrova, Holger Kantz. Modified method of simplest equation and its application to nonlinear PDEs. *Applied Mathematics and Computation* **216**, 2587 - 2595 (2010).

[2] Nikolay K. Vitanov. Modified method of simplest equation: Powerful tool for obtaining exact and approximate traveling-wave solutions of nonlinear PDEs. *Communications in Nonlinear Science and Numerical Simulation* **16**, 1176 - 1185 (2011).

[3] Nikolay K. Vitanov, Zlatinka I. Dimitrova, Kaloyan N. Vitanov. Modified method of simplest equation for obtaining exact analytical solutions of nonlinear partial differential equations: further development of the methodology with applications. *Applied Mathematics and Computation* **269**, 363 - 378 (2015).

[4] Nikolay K. Vitanov, Zlatinka I. Dimitrova. Simple Equations Method and Non-Linear Differential Equations with Non-Polynomial Non-Linearity.*Entropy* **23** (12):1624 DOI:10.3390/e23121624 (2021).

Loaded Equation Method for Computational Identification of Time-dependent Convection Coefficient and Source in a Magnetohydrodynamic Flow

J. D. Kandilarov, L. G. Vulkov

This paper deals with the solution by a finite element method (FEM) combined with a loaded equation technique for the estimation of unknown time-dependent convection coefficient and source in 1-D magnetohydrodynamics flow system. In this inverse problem point and integral observations are posed. Nonclassical formulations of the inverse problem are derived. The FEM procedure is analyzed and optimal error estimates are derived. Numerical algorithms solving the arising system of two loaded parabolic equations are proposed. Numerical experiments are discussed.

Design of a System for Bioinformatics Processing of Metagenomic Data

A. Kirilov

The rapid advancements of the means to obtain and store information has lead to the accumulation of large data bases in Metagenomics. Metagenomics is the field of studying genetic material which has been recovered directly from ecological and clinical samples. The data generated by metagenomic experiments are huge and inherently noisy and fragmented. Therefore specialized software tools are needed in order to collect, store and process information as well as for extract results from large data bases. Choosing suitable software, algorithm and tools enables researchers to process observational data sets in order to discover causal relationships or to summarize and present them in new ways that would enable further analysis by experts in the field.

In order to analyze and classify microbial diversity in samples of varying data size, we use the Galaxy software. In order to analyze the samples we use the Amplicon analysis (targeted sequencing) method which is fundamental in Metagenomics. The data are processed in the web-based Galaxy platform and two server system configurations. The data used to test the web-based Galaxy platform and the local server system are taken from the Human Microbiome Project and originate from human fecal samples. They are divided in three test collections in special fasta file format. The parallel efficiency of the three different system configurations for the data used has been studied. The microbial diversity in the samples of varying data size has been studied and classified using the software.

Acknowledgements The work was accomplished with the financial support of the MES by the Grant №DO1-168/28.07.2022 for providing access to e-infrastructure of the NCHDC – part of the Bulgarian National Roadmap on RIs.

Virtual Tours for Museums Environment

H. Klecherova, M. Raykovska

Virtual tours provide a way to access immovable cultural heritage, galleries, exhibitions, or even landscapes and important historical places online. They can be used for a complete presentation of artifacts, stored away in museum funds, and not accessible to the public. Virtual tours can hold an immense amount of data, such as archive photos, videos, drawings, and research info. They can be even used as tourist guides or educational tools.

The following research aims to demonstrate innovative ways for online museum presence by combining augmented and virtual reality. Both techniques are well known and have great potential to be used for scientific purposes and to be applied in various fields and projects. One of the main advantages of the virtual environment is that it can provide unlimited space for information that can be changed and updated over time. Augmented reality on the other hand adds extra value to the content, provoking the visitor's imagination and senses.

The team at IICT-BAS has created several mixed-reality virtual tours of museum exhibitions so far. A 360-degree, 500MP, robotized head was used for the generation of the panoramas, which were later built into a VR tour. Markers and QR codes were placed alongside the exhibitions for the augmented reality content. The museum's staff provided the necessary text and graphics information for a complete personalized presentation for visitors to improve engagement and satisfaction. The results are fully immersive virtual reality exhibitions that can modify the way people access and perceive historical information.

Reverse Engineering of Human Brain Using EEG Recordings

P. Koprinkova-Hristova, Nadejda Bocheva

EEG allows non-invasive measuring of human brain activity. However, the recorded signals are only from the shallow region bellow the scull from the cortex. It represents the average activity of the neurons firing in synchrony, but could not easily specify the spatial distribution of the sources that generate it.
Having in mind that the brain areas have structural connectivity based mainly on the distances between them, we investigate the possibility to use EEG recordings to reconstruct mutual influence of deeper brain areas. For this aim we constructed a 3-dimensional model of main brain areas based on literature data. Connections between these areas are designed using the rule of small world connectivity, i.e. the close are two areas (neurons) the bigger is probability of their mutual influence and hence the stronger connections between them were supposed.
Next, EEG data was fed to the positions of electrodes as input current to the corresponding areas (groups of neurons) and all connections within the designed structure were allowed to change via STDP rule. Thus the achieved after some time connectivity will be altered by the input signals.
We use our initial experimental data from a human performing visual task. The stimulus was presented on the screen and EEG recordings were synchronized with its presence/absence. Our initial results demonstrate how the brain connectivity was influenced by the visual stimulation and thus which areas are responsible for conscious visual perception.

Acknowledgements The work is partially supported by the Bulgarian Science Fund under the project "Modelling post-perceptual stages of cognitive processing and conscious representations of visual information" No KP-06-N52/6 from 12.11.2021

Concentration-Dependant Behaviour of AMPs in Solution

E. Lilkova, P. Petkov, N. Ilieva, L. Litov

Antimicrobial peptides (AMPs) are promissing candidates for therapeutic alternatives of conventional antibiotics. They are small natural proteins, produced by all types of organisms as part of the nonspecific innate immunity. AMPs display a wide range of antimicrobial, antifungal, antiviral, and even anticancer effects. Usually they are cationic and amphiphilic, however, their mechanism of antimicrobial action is not yet fully understood.
Naturally, AMPs are secreted as part of multicomponent secretory fluids, i.e. sweat, saliva, mucus, etc. It is those mixtures of various peptides and other compounds that exhibit the antimicrobial activity. The behavior of the AMPs in these bodily liquids prior to attacking the target membrane is still an open question.
Here, we employ long-scale molecular dynamics simulations of different linear putative AMPs, isolated form the mucus of the garden snails *Helix Aspersa*, in mono- and multicomponent solutions, as to study *in silico* their behavior in the bodily fluids before their attack on the bacterial membrane. The peptide monomers quickly aggregate into nano-sized clusters that resemble the structure of globular proteins, i.e. a non-polar hydrophobic core covered by solvent-exposed charged and polar residues shell. These clusters actually represent a perfect transport system – locking the hydrophobic uncharged residues in the core of the cluster prevents the interaction with the uncharged eukaryotic membranes, and positioning the charged residues on the cluster surface enables electrostatic interaction with the pathogenic membrane. In addition, the aggregation process promoted folding of some peptide chains due to the the amphiphilic structure in the clusters. This allows for an increase of the local concentration of AMPs to be delivered to the target membrane in a functionally active conformation.

Acknowledgments This work is partially supported by the Bulgarian Science Fund (Grant KP-06-OPR 03-10/2018). Computational resources were provided by the BioSim HPC Cluster at the Faculty of Physics at Sofia University “St. Kl. Ohridski”, Sofia (Bulgaria) and by CI TASK (Centre of Informatics – Tricity Academic Supercomputer & networK), Gdansk (Poland).

Searching Optimal Solutions for Multidimensional Nonlinear Functions in LibreOffice

G. Mateeva, D. Parvanov, T. Balabanov

Introduction There are many types of optimization tasks in actual practice. Many efficient numerical methods have been developed for linear optimization problems (linear objective function and linear constraints). Serious difficulties arise when optimization problems contain some form of nonlinearity. There are infinite possibilities for the participation of nonlinear functions in nonlinear optimization problems, but even the simplest nonlinearity (for example, second-degree) creates enough difficulties. Four viral test functions (Rastrigin, Sphere, Rosenbrock, Styblinski-Tang) have been selected for the needs of the present scientific study. These four functions are characterized by the fact that they can be calculated at a significant value for the dimensions (axes in multidimensional space). The search for optimal and suboptimal values is performed with LibreOffice Calc Nonlinear Solver. Currently, there is a medium-term plan by the team developing the solver to rewrite it in the C++ programming language completely. Despite these efforts, this refinement is not yet complete, and current versions of the office suite use a Java solver that implements a hybrid global heuristic optimization algorithm. The hybrid algorithm includes Differential Evolution and Particle Swarm Optimization. This research aims to determine the performance of the currently used nonlinear solver in LibreOffice Calc. The experiments performed and the results obtained would be extremely useful when the C++ version of the solver is completed, and it is necessary to validate its effectiveness. The report's structure is as follows: Part one is an introduction; Part two introduces the hybrid algorithm embedded in the LibreOffice Calc Nonlinear Solver; Part three is devoted to the experiments conducted and some of the results obtained; Part four contains a conclusion and recommendations for future research.

Hybrid Global Optimization Algorithm The LibreOffice Calc office suite provides options for using several non-linear optimization algorithms. The DEPSO solver has proven to be the most effective for solving non-linear optimization problems over the years. The DEPSO hybrid algorithm uses two meta-heuristic algorithms for global optimization - Difference Evolution and Particle Swarm Optimization. Both algorithms are population-based, with the DE falling under the group of genetic algorithms. The activation of each of the two algorithms happens randomly, with a predetermined probability. By implication, the two algorithms are used with a 50/50 chance. DE is a global optimization algorithm that relies on attempts to improve already available candidate solutions. A numerical evaluation is relied on to what extent these solutions are acceptable to improve candidate solutions. The algorithm does not rely on a gradient and allows use in problems with the extremely high dimensionality of the variable space. Since the algorithm is stochastic, it does not guarantee to reach the global optimum. It is characteristic of the DE that it finds its most practical application in continuous spaces. The optimization process is performed with a set of candidate solutions called a population. From these decisions, parents are selected, and offspring are created. Individuals with a better estimate obtained by calculating the objective function

remain in the population. Recombination of parents most often occurs using crossover and mutation operations. A fundamental difference in the DE from GA is that the mutation occurs on all elements of the corresponding vector, not only on a single piece. PSO is a global optimization algorithm that relies on candidate solutions. Solutions are visualized as particles moving through variable space. Motion is described with current position and velocity. PSO is strongly influenced by the available local best good solution and the known global best solution. Both (local and global) solutions are updated if better ones are found in the optimization process. For the implementation of PSO, no prior knowledge of the task is required, and the usage can be in a black-box fashion. It is characteristic of the PSO and the DE that is usable for high-dimensional problems. It also doesn't need a gradient. Both algorithms, as implemented in LibreOffice Calc, have a series of configuration parameters used with their default values in the present research.

Experiments & Results All experiments were performed on a desktop computer configuration Intel Core i5 2.3GHz, 1 CPU 2 cores, 8GB RAM, operating system macOS High Sierra 10.13.6, and office suite LibreOffice 7.2.7.2. Independent experiments were performed for each of the four functions. Each of the four functions was used at the following dimensions: 1, 5, 10, 50, 100, 500, and 1000. For more than 1000 dimension space, LibreOffice Calc's performance becomes so slow that it does not allow obtaining results in an acceptable computational time for the desktop computer configuration. For all four functions, the computational time (limited to a maximum of 2000 optimization cycles) increases exponentially, in direct proportion to the increase in dimensions in the multidimensional space. The solver finds solutions close to the global optimum for all four functions, up to 100-dimensional space. This result shows that reaching the global optimum becomes difficult with the sharp increase in dimensions. For three functions, up to 100-dimensional space, the dictionary stagnates and does not use the previously pledged 2000 optimization cycles. The only exception is the spherical function, where it ends up stagnating up to about 500 dimensions. The resulting measurements are strongly influenced by how functions are represented in LibreOffice Calc. For each dimension, a value is calculated using a formula on a separate row in the worksheet. They are calculating a large number (in the worst case, 1000) of formulas and summing them to get a single target cell, resulting in a significant delay. The computation time taken in the higher dimensions is due mainly to the mechanism by which the spreadsheet calculates the formulas and not so much to the difficulty in computing the test functions themselves.

Conclusions This research presents results for the efficiency achieved in LibreOffice Calc Nonlinear Solver. Experiments to establish this effectiveness are based on four well-known test functions. The results show that as the variable space dimensionality increases, the optimization module's ability to determine the global optimum also decreases. A second significant conclusion from the obtained results is that the efficiency of the optimization module is highly dependent on the initial point that serves as a starting point when starting the optimization process. Future research directions include exploring the other non-linear optimization modules in LibreOffice Calc and the C++ module currently under development.

Acknowledgments This research is supported by the Bulgarian National Science Fund with the project "Mathematical models, methods and algorithms for solving hard optimization problems to achieve high security in communications and better economic sustainability", KP-06-N52/7/19-11-2021.

Modeling the Interaction of SARS-COV-2 NSP13 with Human TBK1

T. Nedeva, M. Rangelov, N. Hristova, E. Lilkova, P. Petkov, N. Ilieva, L. Litov

COVID-19 is primarily caused by the SARS-CoV-2 virus. As a result of its invasion, the host organism suffers excessive proinflammatory cytokine production and release. Since JAK signalling is crucial for the host's ability to fight against viruses, treating this condition with JAK inhibitors carries the risk of both enhancing viral infection and suppressing the proinflammatory cytokine storm. As found by [Fung, SY. et al. Cell Biosci 12, 36 (2022).],transcriptional activity induced by type I and type II IFN-responsive enhancer elements is reduced by the expression of SARS-CoV-2 NSP13. Thus, NSP13 is capable of suppressing type I IFN production and signaling. NSP13 suppresses type I IFN production by inhibiting the phosphorylation and activity of TBK1-IKKε complex.

In this study, we investigated interactions of SARS-CoV-2 NSP13 with tank-binding kinase 1 (TBK1) by means of molecular dynamics simulations. The initial orientation of SARS-CoV-2 NSP13 with respect to the TBK1 monomer was constructed taking into account the structural similarity between TBK1 SDD and NSP8 after analysis of SARS-CoV-2 Replicase-Transcriptase Complex (RTC). The molecular dynamics simulations were carried out by GROMACS simulaiton package. The analysis of the resulting trajectory revealed a stable complex formation after NSP13 reoriented in the beginning. The stable complex structure was extracted from the trajectory by means of cluster analysis. After its energy minimisaton, the amino acid residues that are crucial for the binding were identified by using Ligplot+, namely ten hydrogen bonds and seven hydrophobic contacts.

The resulting complex will be used further in a search for drugable sites in NSP13 as well as potential drug candidates, such that block the SARS-CoV-2 inhibition of IFN signaling.

Acknowledgements This work was supported in part by the Bulgarian National Science Fund under Grants KP-06-DK1/5/2021 SARSIMM. Computational resources were provided by the BioSim HPC Cluster at the Faculty of Physics at Sofia University "St. Kl. Ohridski", Sofia (Bulgaria) and by CI TASK (Centre of Informatics – Tricity Academic Supercomputer & networK), Gdansk (Poland).

Several Solitary Wave Solutions of the Kdv - Type Equation via Simple Equations Method (SEsM)

E. V. Nikolova

We apply the Simple Equations Method (SEsM) for obtaining exact traveling wave solutions of the fifth–order Korteweg - deVries (KdV) equation. We present the solution of this equation as a composite function of two functions of two independent variables. The two composing functions are constructed as finite series of the solutions of two simple equations. For our convenience, we express these solutions by special functions V, which are solutions of appropriate ordinary differential equations, containing polynomial non–linearity. Various specific cases of the use of the special functions V are presented depending on the highest degrees of the polynomials of the used simple equations. We choose the simple equations used for this study to be ordinary differential equations of second order. On the basis of this choice, we obtain various traveling wave solutions of the studied equation presented by the special functions V, which are solutions of the elliptic equation of Jaccobi and the function $1/cosh^m(\mu x + \nu t)$. Illustrative examples of these solutions are presented. They include different multi-solitons types depending on the numerical values of the free parameters in the solutions chosen for the simulations.

Sum of Powers. Bernoulli Numbers in Terms of Stirling Numbers.

I. Nikolova, P. Marinov

In this paper we solve the famous problem $\sum_{i=1}^{n-1} i^k$ in the basis n^l. We use the following approach. Change the basis in i^k into the basis $(i)_k$ using Stirling numbers. Then solve the problem in the basis $(i)_k$ and return into the original basis i^k using again Stirling numbers. As a consequence we solve the problem represent the Bernoulli numbers in terms of Stirling numbers. Here we use the notation $(i)_k = i(i+1)(i+2)\dots(i+k-1)$
Using induction we prove that:

$$\sum_{i=1}^{n}(i)_k = \frac{(n)_{k+1}}{k+1}\,.$$

Also, we use

$$i^k = \sum_{j=1}^{k}(-1)^{k-j}\left\{ {k \atop j} \right\}(i)_j\,.$$

where with $\left\{ {k \atop j} \right\}$ we denote the Stirling numbers of second kind. Here we use the notation suggested by D. Knuth.

$$\left\{ {k \atop 1} \right\} = 1\,, \qquad \left\{ {k \atop k} \right\} = 1\,.$$

$$\left\{ {k \atop j} \right\} = j\left\{ {k-1 \atop j} \right\} + \left\{ {k-1 \atop j-1} \right\}\,.$$

Since in the literature the above sums are taken in the borders from one till $n-1$ in solving the change of basis backwards from $(i)_k$ to the i^k we are going to use the same borders, i.e.:

$$\sum_{i=1}^{n-1} i^k = \sum_{j=1}^{k}(-1)^{k-j}\left\{ {k \atop j} \right\}\frac{(n-1)_{j+1}}{j+1}$$

The above formula proves that sought sum is a polynomial of n.
For $j=1$

$$(n-1)(n)_1 = n^2 - n\,.$$

and for $j \geq 2$ we get that:

$$\begin{aligned}
(n-1)_{j+1} &= & &(n-1)(n)_j \\
&= & n^{j+1} &+[\sigma_1(1,2,\dots,j-1) - \sigma_0(1,2,\dots,j-1)]n^j \\
& & &+[\sigma_2(1,2,\dots,j-1) - \sigma_1(1,2,\dots,j-1)]n^{j-1} \\
& & &\vdots \\
& & &+[\sigma_{j-1}(1,2,\dots,j-1) - \sigma_{j-2}(1,2,\dots,j-1)]n^2 \quad -(j-1)!\,n\,.
\end{aligned}$$

where by $\sigma_j(a,\cdots b)$ we denoted the elementary symmetric functions of the elements in the parentheses of order j. But the zero in the argument list leads to a simplification of the formulae.

$$\begin{aligned}
\sigma_1(0,1,2,\cdots,j-1) &= \sigma_1(1,2,\cdots,j-1)\\
&\vdots\\
\sigma_l(0,1,2,\cdots,j-1) &= \sigma_l(1,2,\cdots,j-1)\\
&\vdots\\
\sigma_{j-1}(0,1,2,\cdots,j-1) &= \sigma_{j-1}(1,2,\cdots,j-1) = (j-1)!\\
\sigma_j(0,1,2,\cdots,j-1) &= 0\,.
\end{aligned}$$

Now substitute $(n-1)(n)_j$ with its equal we can receive that

$$\begin{aligned}
\sum_{i=1}^{n-1} i^k &= \sum_{j=1}^{k}\frac{(-1)^{k-j}}{j+1}n^{j+1} - \sum_{j=1}^{k}\frac{(-1)^{k-j}}{j+1}\left\{\begin{matrix}k\\ j\end{matrix}\right\}(j-1)!\,n + \sum_{l=1}^{k-1}\sum_{j=1}^{k-l}\frac{(-1)^{k-j-l}}{j+l+1}\times\\
&\quad\times\left\{\begin{matrix}k\\ j+l\end{matrix}\right\}\left[\sigma_l(1,2,\cdots,j+l-1) - \sigma_{l-1}(1,2,\cdots,j+l-1)\right]n^{j+1}\,.
\end{aligned}$$

But in [Vinograd,*Math. encyclopedia*] one can find another formula for the above sum, namely

$$\sum_{i=1}^{n-1} i^k = \frac{1}{k+1}\sum_{j=0}^{k}\binom{k+1}{j}B_j n^{k+1-j}$$

Substituting j by $k+1-j$ we get that:

$$\sum_{i=1}^{n-1} i^k = \frac{1}{k+1}\sum_{j=1}^{k+1}\binom{k+1}{j}B_{k+1-j}n^j =$$

$$= \frac{1}{k+1}\binom{k+1}{1}B_k n + \frac{1}{k+1}\sum_{j=2}^{k+1}\binom{k+1}{j}B_{k+1-j}n^j$$

In the above expressions we denote by B_k the sequence of the Bernoulli numbers. Comparing the two coefficients in-front of n^1 we obtain the following explicit expression for the Bernoulli numbers for $k \geq 1$:

$$B_k = \sum_{j=1}^{k}(-1)^{k-j+1}\left\{\begin{matrix}k\\ j\end{matrix}\right\}\frac{(j-1)!}{j+1}\,.$$

On the Performance and Scalability of the Supercomputer Implementation of the Danish Eulerian Model on the Petascale Supercomputer DISCOVERER and Some Applications

T. Ostromsky

Motivation. The large scale environmental modelling (and air pollution modelling in particular) is one of the toughest problems of computational mathematics (together with the meteorological modelling). All relevant physical and chemical processes in the atmosphere should be taken into account, which are mathematically represented by a complex system of partial differential equation s (PDE). In order to simplify the original PDE system proper splitting procedure is applied. As a result, the initial system is replaced by several simpler systems (submodels), connected with the main physical and chemical processes. Even in case we have to do a local study of the environment in a relatively small area, the model should be calculated in a large spatial domain, because the pollutants can be moved quickly on long distances, driven by the atmosphere dynamics, especially on high altitude. One major source of difficulty is the high intensity of the atmospheric processes, which require a small time-step to be used in order to get a stable numerical solution (at least, as far as the chemistry submodel is concerned). All this makes the treatment of large-scale air pollution models a tuff and heavy computational task, that requires efficient numerical algoritms. It has always been a serious challenge, even for the fastest and most powerful state-of-the-art supercomputers. Fortunately, Bulgaria is one of the leading countries in Eastern Europe with respect to the supercomputer infrastructure development in the recent years.

The supercomputer DISCOVERER. After the IBM Blue Gene/P (installed in BSC/NCSA in 2008, now retired) and the Avitohol system (produced by Hewlett-Packard, installed in IICT-BAS in 2015, still operational), Discoverer is the third Bulgarian supercomputer ranked in the TOP500 list of the most powerful supercomputers in the world and the first with computing power above 1 petaflops. and the first with computing power measured in petaflops*. The performance of the machines to enter this list is evaluated through special tests carried out according to the standards and requirements of the independent non-governmental organisation that compiles the list. Discoverer's test results exceeded 4.5 petaflops and so it was ranked 91st on the TOP500 world's most powerful supercomputer systems list (and 27th most powerful in the European Union) by the time of its installing – the summer of 2021. The machie is located in Sofia Tech Park and has been installed by Atos company with the support of the consortium "Petascale Supercomputer – Bulgaria". It is a part of the international project for creation of powerful network of high-performance machines of the EuroHPC Joint Undertaking.
The system is based on the BullSequana XH2000 platform (CPU type – AMD EPYC 7H12 / 2.6GHz, 280W) and has 1128 nodes with 144384 cores in total (128 cores per node, 128 GB RAM per node). The total RAM of the system is 300 TB, the total disk storage – about 2 PB.

The Danish Eulerian Model. A large-scale environmental model - the Danish Eulerian Model (DEM) was implemented on the new petascale supercomputer DISCOVERER, installed last year by Atos Company in Sofia Tech Park, Bulgaria. The machine is part of the emerging supercomputing network under development by the European High-Performance Computing Joint Undertaking (EuroHPC JU). DEM is mathematically represented by a system of partial differential equations for calculating the concentrations of a number of pollutants in the atmosphere above a large geographical region (including the European continent, the Mediterranean and parts of Asia, North Africa and the Atlantic ocean). The main physical and chemical processes (horizontal and vertical wind, diffusion, chemical reactions, emissions and deposition) are adequately represented in the system. The MPI standard library is used as a main parallelization tool. MPI parallelization is based on the space domain partitioning. The space domain is divided into sub-domains and each MPI task works on its own sub-domain. On each time-step there is no data dependency between the MPI tasks on both the chemistry and the vertical exchange stages. This is not so on the advection-diffusion stage. Spatial grid partitioning between the MPI tasks requires overlapping of the inner boundaries and exchange of certain boundary values on the neighbour subdomains for proper treatment of the boundary conditions. The subdomains are usually too large to fit into the fastest cache memory of the corresponding CPU. In order to achieve good data locality, the smaller calculation tasks are grouped in chunks (if appropriate) for more efficient cache utilization. This is done in order to reduce the data transfer between the cache and the main (slower access) memory. The size of chunks should be tuned with respect to the cache size of the target machine.

Applications. DEM is a powerful and flexible air pollution model, which produces a huge amount of output results in quite reasonable time, if powerful supercomputers are used to run it. It is capable of calculating the levels of concentration for a number of dangerous pollutants and other chemically active species interacting with them (precursors), over a long time period. Moreover, various accumulative quantities (AOT40, AOT60, etc.) can be calculated on yearly basis, which have significant impact in the area of agriculture (on the yield of crops in particular), forestry, wildlife and human health. The model results can be used in different long-term environmental studies and simulations as follows:

- Air pollution evaluation and protection measures;
- Human healthcare;
- Economics of agriculture (yield & losses of crops estimation);
- Forestry and wildlife protection;
- Global climate changes consequences simulation;
- Simulation of industrial accidents and natural disasters.

It has been successfully applied in many scientific and practical problems in various important areas (environmental, medical, social, economic, etc.).

Acknowledgements This research was supported in part by the Bulgarian NSF project "Efficient methods for modelling, optimization and decision making" (contract # KP-06-N52/5), by the Petascale-Bulgaria Supercomputer Consortium and EuroHPC JU.

References

[1] Ø. Hov, Z. Zlatev, R. Berkowicz, A. Eliassen and L. P. Prahm, Comparison of numerical techniques for use in air pollution models with non-linear chemical reactions, Atmospheric Environment 23 (1988), pp. 967–983.

[2] Tz. Ostromsky, I. Dimov, R. Georgieva, Z. Zlatev, Air pollution modelling, sensitivity analysis and parallel implementation, *Int. Journal of Environment and Pollution*, Vol. 46 (1-2), (2011), pp. 83–96.

[3] Tz. Ostromsky, Z. Zlatev, Parallel Implementation of a Large-scale 3-D Air Pollution Model, in: Large Scale Scientific Computing (S. Margenov, J. Wasniewski, P. Yalamov, Eds.), LNCS-2179, Springer, 2001, pp. 309–316.

[4] WEB-site of the Danish Eulerian Model, available at:
http://www.dmu.dk/AtmosphericEnvironment/DEM

[5] Z. Zlatev, Computer treatment of large air pollution models, Kluwer (1995).

[6] Z. Zlatev, I. Dimov, Computational and Numerical Challenges in Environmental Modelling, Elsevier, Amsterdam (2006).

CNN Computing of Double Sine-Gordon Equation with Memristor Synapces

A. Slavova, R. Tetzlaff

In this talk we shall study double Sine-Gordon equation with memristor synapses. The physical object is quantum of magnetic flow, called fluxon. Fluxons are stable in the sense that they can be conserved, their direction can be changed and they can contact electronic devices. Their advantage is that they process information with a very high speed and with a very low energy supply. For this reason, fluxons have applications in information processing of electronic devices. In fact fluxons arise in the well known Josephson Junction (JJ) which is used in many applications in superconductor electronics.Recently, JJ have been considered as a source of THz radiation. Fluxons moving coherently in such junctions are a possible source of radiation.
The relation between Cellular Neural Network (CNN) and the Josephson Transmission Line (JTL) array has been studied in the literature [1-3]. Two-dimensional array of Josephson Junctions is considered in [1]. Authors report the results of a Floquet analysis of such arrays of resistively and capacitively shunted JTLs in an external transverse magnetic field. The Floquet analysis indicates stable phase locking of the active junctions over a finite range of values of the bias current and junction capacitance, even in the absence of an external load.
In this talk we shall study the CNN computing of kink and kink-anti-kink interactions arising in double Sine-Gordon CNN model with memristor synapses. We shall present theoretical and simulation results.

References

[1] L. Fortuna, M.Frasca, A.Rizzo, Self-organizing behavior of arrays of non identical Josephson junctions, 2002 IEEE International Symposium on curcuits and systems, 5:213- 216, 2002.
[2] B.D. Josephson, Weakly coupled super-conductors, in: Superconductivity, ed. by R.D.Parks, Marcel Dekker, New York,423-448.
[3] B.Trees, D.Stround,Two-dimensional arrays of Josephson junctions in a magnetic field: a stability analysis of synchronised states, Physical Review B,59:10:7108-7115, 1999.

An Investigation of Voluntary Saccadic Eye Movements During the Presentation of Color Visual Images in Different Parts of the Full Screen Visual Field

M. Staneva, M. Iliev

The present work investigates the influence of semantic priming on the characteristics of voluntary saccades during visual image analysis.
We used the experimental results from our previous studies applying semantic priming (Bock et al , 2014, Staneva et al, 2018; Staneva & Grigorova, 2019) before and after the adaptation of reactive saccades to examine whether the characteristics of voluntary saccades are affected by the immediate application of broad attentional priming.
The subject was seated at 60 cm from a 27-inch screen with a resolution of 1366 x 768 pixels, with the head fixed using a chin rest. After initial calibration, the eye movements were recorded using the Eye Tracker GP3HD at 150 Hz.
A new software tool was developed in the Python programming language to assist in extracting the following eye-movement parameters:

1. The total duration of all fixations from the start of the recording in seconds;
2. The duration of single fixations in seconds;
3. The saccade magnitude;
4. The saccade direction.

The visual scene was divided into pieces on the screen. In each of them, in a pre–defined order, appeared a target replaced by an image after a fixed delay. The experiment started with presenting a target in the screen center for 3 seconds. After a delay of 3 seconds, a visual stimulus picture appears, occupying the entire screen. The presentation of each image continues for 15 seconds.
The presentation consists of 16 images, which are calibrated and equalized on brightness, contrast and resolution. The instructions to the subjects were to direct their gaze to the center of the targets and look at the details as much as possible. 10 healthy people and 10 glaucoma patients, aged 20 - 60 years, took part in the study.
The examined people are first looking at 8 images. After a short break, they also complete an association task using semantic priming. The subjects in the experiment were also instructed to mentally arrange five jumbled words into a sentence and cross out the redundant illogical word from the list of words. The word's meaning was related to open space concepts. The time for handwriting twenty consecutive sentences on the sheet was recorded for each subject separately, with an average result of 10 minutes.
After finishing the priming, the examined subjects are looking at another 8 images. After that they fill out a card with the order of shown images and the presence or absence of certain objects described in a questionnaire. The time it takes to fill out the card is recorded and also the correct answers.

Hypothesis:
The application of priming with a winde focus of attention on the images with equalized brightness and contrast:

1. improves the analysis of amount of images when observing visual stimulus;
2. helps the vision system to choose a cognitive strategy, which makes the most effective visual path in a more detailed recognition of the images.

Results:
The temporal saccadic characteristics were transformed in advance to remedy distribution skewness. The results of the analysis show that the addition of priming with a wide focus of attention on the visuals influences the analysis of recognising similar forms in terms of the average continuation of fixation in seconds. With the addition of priming tendencies can be observed with influence on the analysis of visual stimulus on the same forms in terms of:

1. the average continuation of fixation in seconds;
2. decrease in amount of saccades, continuation of fixation and increase of the amplitude;
3. change in the distribution and amount of directions of the saccades;
4. the recorded correct answers and mistakes in the questionnaire and time it took to fill it out.

The results also revealed tendencies of the participant's age and interaction between the age of the subjects, and the latency of the first saccade and the fixation. The results of this preliminary study show that priming changes the preparation time of voluntary saccades and affects the characteristics of eye movements in scene exploration. Further exploration of its influence with a larger group of participants is pending.

Acknowledgments This work contains results, which are supported by the BAS – Institute of Neurobiology project FNI-3028/KP-06-PM43/6/22.12.2020 and the UNWE project for scientific researchers with grant agreement No. NID NI–11/2022.

Analytical Modelling & Experimental Testing of Advanced Ransomware

S. Tafkov, Z. Minchev

Modern cybersecurity trends are nowadays addressing a rising peak of ransomware attacks. This phenomenon is getting even more complicated with machine learning advancements, taking already a dark web paid solution, known as Ransomeware as a Service, which is quite profitable, especially with corporate environments attacks [1]. The biggest problem so far is the proactive behavioral analysis necessity that needs an adequate modelling and analysis and actually is quite difficult for achieving due to different families of ransomware constant appearance. In brief, there could be identified two main types of ransomware families - standard & smart ones, encrypting the user data with different solutions, usually symmetric, though asymmetric ones are also possible, but have mainly a destructive nature [2]. The study presents an analytical modelling of both cyberattacks and defense scenarios [3], with dual (independable & dependable) context perspectives. A graph-based preliminary risk assessment, following some of the ideas of [4] is performed, providing details on the system of interest bottlenecks in distributed (local and remote) architectures [5]. Further, the obtained results are extended with real-world experimental tests, that give in fact some corrections on the initial risks expectations. The study actually tries to identify the balance in the natural vs artificial intelligence implementation with smart machine learning algorithms. Thus, giving in this manner a better outlook to the cybersecurity risk proactive identification level within the future post-information age of hybrid human-machine knowledge, towards an autonomous and evolutionary security environment for the new digital age.

References

[1] 2022 Data Breach Investigations Report, Verizon, 2022. [Online]. https://www.verizon.com/business/resources/reports/dbir/. [Accessed: 15-Dec-2022].

[2] S. Tafkov, Z. Minchev, Advanced Cyber Risks for Computer Systems with Future Ransomware Attacks, In Z. Minchev (Ed) Digital Transformation in the Post-Information Age, Ch. 6, pp. 99-113, Softtrade & Institute of ICT, Bulgarian Academy of Sciences, 2022.

[3] S. Tafkov, Z. Minchev, Ransomware Detection & Neutralization System, In Proc. of X International Scientific Conference Hemus 2020 Research and Investment in Technology Innovation – A Crucial Factor for Defence and Security, Defence Institute "Prof. Tsvetan Lazarov", Bulgaria, 2021, pp. II-144-II-152, DOI:10.13140/RG.2.2.21029.12009.

[4] Z. Minchev, Malicious Future of AI: Transcendents in the Digital Age, in Proc. of 12th International Conference on Business Information Security (BISEC-2021), Belgrade, Serbia, December 3rd, pp. 18-22, 2021.

[5] S. Tafkov, Cloud Intelligence Network for Ransomware Detection and Infection Effect Reversing," in Proc. of 12th International Conference on Business Information Security (BISEC-2021), Belgrade, Serbia, December 3rd, pp. 23-26, 2021.

Interdisciplinary Studies of "Kazlacha" Circular Ditches Complex: Photogrammetry, Laser Scanning and 360-Degree Photography for Creating a Digital Archive in KlaDa Bulgaria

G. Vasilev, H. Klecherova, G. Evtimov, M. Raykovska, V. Petrova

The Neolithic complex of circular ditches "Kazlacha" is located in Southeastern Bulgaria, between the villages of Chokoba, Sliven region and Hadzhidimitrovo, Yambol region and it occupies an area of 60 acres. It covers five consecutively built circular enclosures (A, B, C, D, E) that have diameters from 50 to 170 meters and consist of one to four parallel ditches. Such a similar concentration of trench systems dating from the first half of the 6th millennium BC has not been established so far, not only for the Southeast region, but also for the whole of Europe. The research of this rare type of archaeological monument has been carried out regularly since 2020. It is located on private cultivated land, which requires backfilling of the surveyed area after each archaeological campaign. Therefore, the prospects for documentation and socialization require a different approach, related to the creation of three-dimensional models, virtual tours, etc., in order to receive appropriate promotion and distribution through Internet platforms and sites. This implies the use of three-dimensional documentation (laser scanning, photogrammetry, etc.), already implemented in 2021 for the single fence "B" (https://3dlab.iict.bas.bg/vrtours/Kazlacha2021/).

A second interdisciplinary survey was also conducted in September 2022, targeting enclosure "C", which consists of two parallel ditches. The goal is to create a digital archive that will store the data from the archeological studies performed over the years and present them to the scientific audience and the rest of the society through the platform of CLaDa Bulgaria. The methods of three-dimensional documentation have emerged as standard approaches to virtual archeology since the early 21st century and they are rapidly becoming an integral part of regular or salvage archaeological surveys, providing further technological contributions to the visualization of findings and structures.

For the purpose of the present study, the team agreed on laser scanning, 360-degree photography, aerial and close-range photogrammetry for capturing the state of the archeological research at the time of survey.

The possibility of integrating three-dimensional models from different systems reveals new horizons for presenting the archaeological heritage in virtual, augmented or mixed reality, which can be periodically updated with newly gathered data and promote the dissemination of new knowledge.

Edge Convex Smooth Interpolation Curve Networks with Minimum L_∞-norm of the Second Derivative

K. Vlachkova, K. Radev

We consider the extremal problem of convex scattered data interpolation in $\mathbb{R}^3$ by smooth edge convex curve networks with minimal L_p-norm of the second derivative for $1 < p \leq \infty$. The problem for $p = 2$ was set and solved by Andersson et al. (1995). Vlachkova (2019) extended the results in (Andersson et al., 1995) and solved the problem for $1 < p < \infty$. The solution in the case $1 < p < \infty$ is unique for strictly convex data. The minimum edge convex L_p-norm network for $1 < p < \infty$ is obtained from the solution to a system of nonlinear equations with coefficients determined by the data. The approach used in (Vlachkova, 2019) can not be applied to the corressponding extremal problem for $p = \infty$. In this case the solution is not unique.

Here we establish the existence of a solution to the extremal interpolation problem for $p = \infty$. This solution is a quadratic spline function with at most one knot on each edge of the underlying triangulation. We also propose sufficient conditions for solving the problem for $p = \infty$.

Bellow we present the solution for $p = \infty$ to a simple example where the data are obtained from a regular triangular pyramid.

Example 1 We consider the data $(-1/2, -\sqrt{3}/6, 0)$, $(1/2, -\sqrt{3}/6, 0)$, $(0, \sqrt{3}/3, 0)$, and $(0, 0, -1/2)$. The vertices of the associated triangulation T are $V_1 = (-1/2, -\sqrt{3}/6)$, $V_2 = (1/2, -\sqrt{3}/6)$, $V_3 = (0, \sqrt{3}/3)$, and $V_4 = (0, 0)$. The set of indices defining the edges of T is $N_B = \{12, 23, 31, 41, 42, 43\}$. The exact solution $F = \{f_{ij}\}_{ij \in N_B}$ for $p = \infty$ can be found directly by solving the corresponding nonlinear system. It is

$$f_{12}(t) = f_{23}(t) = f_{31}(t) = 3(t^2 - t)/2,\ 0 \leq t \leq 1;$$
$$f_{j4}(t) = 3t^2/2 - \sqrt{3}t,\ 0 \leq t \leq \sqrt{3}/3, \quad j = 1, 2, 3.$$

The L_∞-norm of the second derivative of the solution is $\|F''\|_\infty = 3$. The triangulation T and the corresponding edge convex minimum L_∞-norm network are shown in Fig. 1.

Acknowledgments. This work was supported in part by Sofia University Science Fund Grant No. 80-10-109/2022, and European Regional Development Fund and the Operational Program "Science and Education for Smart Growth" under contract №BG05M2OP001-1.001-0004 (2018-2023).

References

[1] L.-E. Andersson, T. Elfving, G. Iliev, K. Vlachkova. Interpolation of convex scattered data in $\mathbb{R}^3$ based upon an edge convex minimum norm network. *J. Approx. Theory*, 80(3), 299-320, 1995. https://doi.org/10.1006/jath.1995.1020

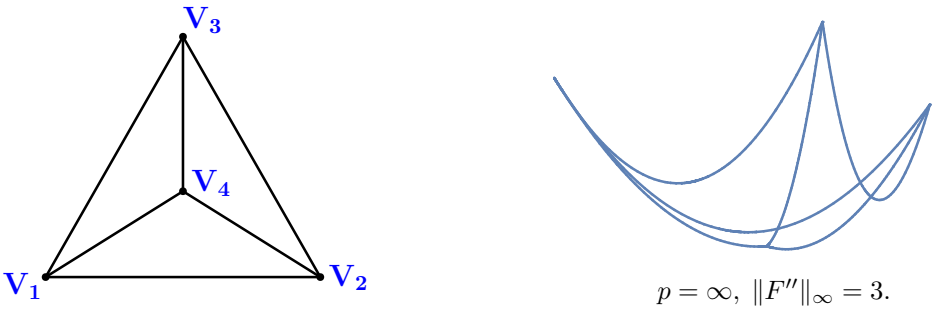

Figure 1: The triangulation T and the corresponding edge convex minimum L_∞-norm network for the data in Example 1.

[2] K. Vlachkova, Interpolation of convex scattered data in $\mathbb{R}^3$ using edge convex minimum L^p-norm networks, $1 < p < \infty$, *AIP Conf. Proc.*, 2183, 070028, 2019. https://doi.org/10.1063/1.5136190

Accounting Service for Southeast Europe Infrastructure: New Developments

S. Yordanov

The accounting service collects, analyzes, and then provides information about the usage of services for example, HPC usage, storage data, virtual machines data, and usage of services. The service provides information only related to NI4OS/EOSC services and is available to the project management team and the service administrators.
In the accounting service, the users are able to browse data represented by tables, charts, and graphs. The collection of usage data is done by the RESTful application programming interface (API), with the ability to be fully automated. The system offers pre-written scripts with installation instructions that automatically post data over certain periods of time. The data collected can then be grouped by country, date, year, name of the resource, name of the application, and research community, with the ability to be filtered and sorted. After that, the data can be exported into CSV or excel formats.
In this talk, I will present about the latest developments of the NI4OS accounting service, which is onboarded in the EOSC platform. I will also describe the service architecture that uses the Flask web framework, which is a popular web framework for building web applications using the Python programming language. It is a microframework that provides only the essential components, making it easy to use and extend. Flask is often used for developing small to medium-sized applications, as it provides a simple and lightweight way to connect the user interface to the backend. One of the key features of Flask is its flexibility. It allows developers to choose the tools and libraries they want to use rather than forcing them to use a specific set of tools. This makes it easy to integrate Flask with other libraries and frameworks, allowing developers to build powerful and complex applications using a wide range of technologies.

Acknowledgment The work was supported by the European Commission through the H2020 Research Infrastructures under the project NI4OS -Europe -National initiatives for open science in Europe (H2020 №857645).

Part B

List of participants

Ivan Bazhlekov
Institute of Mathematics and Informatics
Bulgarian Academy of Sciences
Acad. G. Bonchev Str., Bl. 8
1113 Sofia, Bulgaria
i.bazhlekov@math.bas.bg

Emilia Bazhlekova
Institute of Mathematics and Informatics
Bulgarian Academy of Sciences
Acad. G. Bonchev Str., Bl. 8
1113 Sofia, Bulgaria
e.bazhlekova@math.bas.bg

Vilislav Boutchaktchiev
University of National and World
Economy
1700 Sofia, Bulgaria
vboutcha@unwe.bg
and
Institute of Mathematics and Informatics
Bulgarian Academy of Sciences
Acad. G. Bonchev Str., Bl. 8
1113 Sofia, Bulgaria

Maria Datcheva
Institute of Mechanics
Bulgarian Academy of Sciences
Acad. G. Bonchev Str., Bl. 4
1113 Sofia, Bulgaria
datcheva@imbm.bas.bg

Dimitar Dimitrov
Institute of Information and
Communication Technologies
Bulgarian Academy of Sciences
Acad. G. Bonchev Str., Bl. 2
dimitar.dimitrov@iict.bas.bg

Dimo Dimov
Institute of Information and
Communication Technologies
Bulgarian Academy of Sciences
Acad. G. Bonchev Str., Bl. 2
dimo.dimov@iict.bas.bg

Georgi Evtimov
Institute of Information and
Communication Technologies
Bulgarian Academy of Sciences
Acad. G. Bonchev Str., Bl. 2
georgi.evtimov@iict.bas.bg

Ivan Georgiev
Institute of Information and
Communication Technologies
Bulgarian Academy of Sciences
Acad. G. Bonchev Str., Bl. 2
and
Institute of Mathematics and Informatics
Bulgarian Academy of Sciences
Acad. G. Bonchev Str., Bl. 8
1113 Sofia, Bulgaria
john.g.georgiev@gmail.com

Slavi Georgiev
Ruse University "Angel Kanchev"
8 Studentska Str.
7017 Ruse, Bulgaria
sggeorgiev@uni-ruse.bg

Silvi-Maria Gurova
Institute of Information and
Communication Technologies
Bulgarian Academy of Sciences
Acad. G. Bonchev Str., Bl. 2
smgurova@parallel.bas.bg

Roumen Iankov
Institute of Mechanics
Bulgarian Academy of Sciences
Acad. G. Bonchev Str., Bl. 4
1113 Sofia
iankovr@abv.bg

Mario T. Iliev
Faculty of Physics
Sofia University "St. Kliment Ohridski"
5 J. Bourchier Blvd.
1164 Sofia, Bulgaria
ozo@phys.uni-sofia.bg

Milena Ilieva
Institute of Neurobiology
Bulgarian Academy of Sciences
Acad. G. Bonchev Str., Bl. 23
1113 Sofia
mil_ilieva@abv.bg

Nevena Ilieva
Institute of Information and
Communication Technologies
Bulgarian Academy of Sciences
Acad. G. Bonchev Str, Bl. 25A
1113 Sofia, Bulgaria
nevena.ilieva@iict.bas.bg
and
Institute of Mathematics and Informatics
Bulgarian Academy of Sciences
Acad. G. Bonchev Str., Bl. 8
1113 Sofia, Bulgaria

Radan Ivanov
National Institute of Geophysics,
Geodesy and Geography
Bulgarian Academy of Sciences, Acad. G. Bonchev Str., Bl. 3,
1113 Sofia, Bulgaria
rivanov@geophys.bas.bg

Jivko Jeliazkov
Institute of Mathematics and Informatics
Bulgarian Academy of Sciences
Acad. G. Bonchev Str., Bl. 8
1113 Sofia, Bulgaria
jivko@math.bas.bg

Ivan P. Jordanov
University of National and World
Economy
Studentski Grad, UNWE - office 2087
1700 Sofia, Bulgaria
and
Institute of Mechanics,
Bulgarian Academy of Sciences
Acad. G. Bonchev Str.,Bl. 4
1113 Sofia, Bulgaria
jordanovip@gmail.com

Juri Kandilarov
Ruse University "Angel Kanchev"
8 Studentska Str.
7017 Ruse, Bulgaria
ukandilarov@uni-ruse.bg

Nikola Kasabov
School of Engineering, Computer and
Mathematical Science,
KEDRI, Auckland University of Technology,
St.Paul street, AUT WZ building
1142 Auckland, New Zealand
nkasabov@aut.ac.nz

Alexandar Kirilov
Institute of Information and
Communication Technologies
Bulgarian Academy of Sciences
Acad. G. Bonchev Str., Bl. 2
1113 Sofia, Bulgaria
alex.kirilov@acad.bg

Hristina Klecherova
Institute of Information and
Communication Technologies
Bulgarian Academy of Sciences
29 Filip Makedonski Str.
4002 Plovdiv, Bulgaria
hristina.klecherova@iict.bas.bg

Petia Koprinkova-Hristova
Institute of Information and
Communication Technologies
Bulgarian Academy of Sciences
Acad. G. Bonchev Str., Bl. 2
1113 Sofia, Bulgaria
pkoprinkova@yahoo.com

Hristo Kostadinov
Institute of Mathematics and Informatics
Bulgarian Academy of Sciences
Acad. G. Bonchev Str., Bl. 8
1113 Sofia, Bulgaria
hristo@math.bas.bg

Elena Lilkova
Institute of Information and
Communication Technologies
Bulgarian Academy of Sciences
Acad. G. Bonchev Str., Bl. 25A
1113 Sofia, Bulgaria
elena.lilkova@iict.bas.bg

Pencho Marinov
Institute of Information and
Communication Technologies
Bulgarian Academy of Sciences
Acad. G. Bonchev Str., Bl. 25A
1113 Sofia, Bulgaria
pencho.marinov@gmail.com

Gergana Mateeva
Institute of Information and
Communication Technologies
Bulgarian Academy of Sciences
Acad. G. Bonchev Str., Bl. 2
1113 Sofia, Bulgaria
gmateeva@gmail.com

Zlatogor Minchev
Institute of Information and
Communication Technologies
Bulgarian Academy of Sciences
Acad. G. Bonchev Str., Bl. 25A
1113 Sofia, Bulgaria
zlatogor.minchev@gmail.com

Tsvetina Nedeva
Faculty of Physics
Sofia University "St. Kl. Ohridski"
5 J. Bourchier Blvd.
1164 Sofia, Bulgaria
cvetinanedeva@gmail.com

Elena Nikolova
Institute of Mechanics
Bulgarian Academy of Sciences
Acad. G. Bonchev Str.,Bl. 4
1113 Sofia, Bulgaria
elena@imbm.bas.bg

Tzvetan Ostromsky
Institute of Information and
Communication Technologies
Bulgarian Academy of Sciences
Acad. G. Bonchev Str., Bl. 25A
1113 Sofia, Bulgaria
ceco@parallel.bas.bg

Peicho Petkov
Faculty of Physics
Sofia University "St. Kl. Ohridski"
5 J. Bourchier Blvd.
1164 Sofia, Bulgaria
peicho@phys.uni-sofia.bg

Dimiter Prodanov
Interuniversity Microelectronics
Center (IMEC)
Kapeldreef 75
3001 Leuven, Belgium
dimiter.prodanov@imec.be

Miglena Raykovska
Institute of Information and
Communication Technologies
Bulgarian Academy of Sciences
Acad. G. Bonchev Str., Bl. 2
1113 Sofia, Bulgaria
miglena.raykovska@iict.bas.bg

Miriana Raykovska
Institute of Information and
Communication Technologies
Bulgarian Academy of Sciences
Acad. G. Bonchev Str., Bl. 2
1113 Sofia, Bulgaria
miriana.raykovska@iict.bas.bg

Angela Slavova
Institute of Mathematics and Informatics
Bulgarian Academy of Sciences
Acad. G. Bonchev Str., Bl. 8
1113 Sofia, Bulgaria
slavova@math.bas.bg

Georgi Vasilev
Institute of Information and
Communication Technologies
Bulgarian Academy of Sciences
29 Filip Makedonski Str.
4002 Plovdiv, Bulgaria
georgi.vasilev@iict.bas.bg

Nikolay K. Vitanov
Institute of Mechanics
Bulgarian Academy of Sciences
Acad. G. Bonchev Str.,Bl. 4
1113 Sofia, Bulgaria
vitanov@imbm.bas.bg

Krassimira Vlachkova
Faculty of Mathematics and Informatics
Sofia University "St. Kl. Ohridski"
5 J. Bourchier Blvd.
1164 Sofia, Bulgaria
krassivl@fmi.uni-sofia.bg

Lubin Vulkov
Ruse University
6 Studentska St
7017 Ruse, Bulgaria
lvalkov@uni-ruse.bg

Svetlozar Yordanov
Institute of Information and
Communication Technologies
Bulgarian Academy of Sciences
Acad. G. Bonchev Str., Bl. 25A
1113 Sofia, Bulgaria
svetlozar@parallel.bas.bg